$[Fe(\mu\text{-btzmp})_2(\text{btzmp})_2](ClO_4)_2$: a doubly-bridged 1D spin-transition bistetrazole-based polymer showing thermal hysteresis behaviour†‡

Manuel Quesada,[a] Huub Kooijman,[b] Patrick Gamez,[a] José Sánchez Costa,[a] Petra J. van Koningsbruggen,*[c] Peter Weinberger,[d] Michael Reissner,[e] Anthony L. Spek,[b] Jaap G. Haasnoot*[a] and Jan Reedijk[a]

The reaction of btzmp (1,2-bis(tetrazol-1-yl)-2-methylpropane) with $Fe(ClO_4)_2$ generates a 1D polymeric species, $[Fe(\mu\text{-btzmp})_2(\text{btzmp})_2](ClO_4)_2$, showing a steep spin transition ($T_{1/2}\uparrow = 136$ K and $T_{1/2}\downarrow = 133$ K) with a 3 K thermal hysteresis. The crystal structure at 100 and 200 K reveals that, in contrast to other bistetrazole based spin-transition systems such as $[Fe(endi)_3](BF_4)_2$ and $[Fe(btzp)_3](ClO_4)_2$, the present compound has only two ligands bridging the metallic centres, while the other two coordination positions are occupied by two mono-coordinated (non-bridging) btzmp ligands. This peculiarity confers an unprecedented crystal packing in the series of 1D bistetrazole based polymers. The change in spin state is accompanied by an order/disorder transition of the ClO_4^- counterion. A careful examination of the structural changes occurring upon the spin transition indicates that this order/disorder is most likely affected by the modification of the [tetrazole-centroid]–N_D–Fe angle (which is typical of bistetrazole spin-transition materials). Apart from X-ray analysis, also magnetic susceptibility, Mössbauer and UV-vis spectroscopies have been used to characterise the HS and the LS states of $[Fe(\mu\text{-btzmp})_2(\text{btzmp})_2](ClO_4)_2$.

Introduction

The spin-crossover (SCO) phenomenon in iron(II) compounds discovered in the 1960's has since then been greatly developed due to the potential technological applications.[1] The transition between the $^1A_{1g}$ low spin state and the $^5T_{2g}$ high spin state can be triggered by temperature, pressure or light.[2] Although molecular in nature (observed in solution),[3] the phenomenon is greatly affected by cooperative effects,[4] which determine the character of the thermally-induced transition. Thus, steep, gradual, stepwise, or incomplete transitions presenting a hysteresis may be observed. Among them, compounds showing abrupt transitions, or those presenting hysteresis behaviour are the most promising materials for future applications.

The degree of cooperativity depends on the capacity of a material to convey, through elastic interactions,[5] the molecular changes occurring upon the transition. Highly cooperative materials are responsible for the observation of steep (with or without hysteresis) transitions.[2] Phase changes or order/disorder phenomena have also been pointed out as causes for some of the abrupt transitions observed.[6] Two strategies, namely the supramolecular and polymeric approaches, are currently applied to develop new cooperative spin-crossover systems. The first approach uses π–π interaction and/or hydrogen bonds as paths for the communication between the metal centres. In polymeric SCO materials, the covalent nature of the links between the metal centres is intended to enhance the communication.[7–10] Both strategies are aimed at obtaining overall rigid crystal lattices through which the information can be efficiently transmitted.[11]

Bistetrazole-based SCO materials are well-known polymeric systems which present various types of transitions; from gradual to steep with hysteresis. $[Fe(btzp)_3](ClO_4)_2$ (btzp = 1,2-bis(tetrazol-1-yl)propane) was the first 1D SCO polymer to be crystallised and shows a gradual spin transition.[12] The flexibility of the spacer, and thus of the overall crystal lattice was suggested as the reason for such a lack of cooperativity. A similar behaviour is observed for the endi (1,2-bis(tetrazol-1-yl)ethane) derivative.[13] The increase of the length of the alkyl spacer to four carbons in the btzp (1,4-bis(tetrazol-1-yl)butane) ligand, surprisingly yields an iron(II) compound exhibiting a steeper transition. Although the linker between the tetrazoles is longer and thus structural flexibility is *a priori* expected, the interlocked 3D network of the material generates rigidity.[11,14] Moreover, the size of the cavities in the crystal lattice match the size of the PF_6^- anions, creating a compact crystal packing. This is further confirmed with the perchlorate analogue, whose smaller size of the counterion yields a 3D

[a]*Leiden Institute of Chemistry, Gorlaeus Laboratories, Leiden University, P.O. Box 9502, 2300-RA, Leiden, The Netherlands. E-mail: haasnoot@chem.leidenuniv.nl; Fax: +31-71-5274671; Tel: +31-71-5274459*
[b]*Bijvoet centre of Biomolecular Research, Crystal and Structural Chemistry, Utrecht University, Padualaan 8, 3584-CH, Utrecht, The Netherlands; Fax: +31-30-2533940; Tel: +31-30-2532538*
[c]*Stratingh Institute for Chemistry University of Groningen, Nijenborgh 4, 9747-AG, Groningen, The Netherlands. E-mail: p.j.van.koningsbruggen@rug.nl; Fax: +31-50-3634363*
[d]*Institute of Applied Synthetic Chemistry, Vienna University of Technology, Getreidemarkt 9/163-AC, A-1060, Vienna, Austria; Fax: +43-1-58801-16299; Tel: +43-1-58801-15352*
[e]*Institute of Solid State Physics, Vienna University of Technology, Wiedner Hauptstrasse 8-10/138, A-140, Vienna, Austria; Fax: +43-1-58801-13898; Tel: +43-1-58801-13772*
† CCDC reference numbers 650322–650324. For crystallographic data in CIF or other electronic format see DOI: 10.1039/b709460d
‡ Electronic supplementary information (ESI) available: Further experimental details. See DOI: 10.1039/b709460d

spin-transition network with a more gradual transition[15] or a steep but very incomplete transition,[16] depending on the solvent used. The systematic study carried out by Weinberger *et al.* on the variation of the length of the alkyl-spacer revealed that the length and parity of the linker not only affect the cooperativity of the system, but also the transition temperature.[15]

The new ligand btzmp (1,2-bis(tetrazol-1-yl)-2-methylpropane, Fig. 1), which represents the next logical step in the endi–btzp series, is herein presented. So, two methyl substituents are now included in the ethane bridge (Fig. 1). The effect of this additional methyl substituent on the structural arrangement of the complex [Fe(μ-btzmp)$_2$(btzmp)$_2$](ClO$_4$)$_2$ (**1**) is studied by means of single crystal X-ray diffraction. Magnetic susceptibility measurements, ^{57}Fe Mössbauer and UV-vis spectroscopy are used to investigate the spin-transition properties of the material. The drastic influence of the extra methyl group on the spatial arrangement in the solid-state structure of the corresponding material, which consequently affects its magnetic behaviour is discussed in comparison with the endi and btzp derivatives.
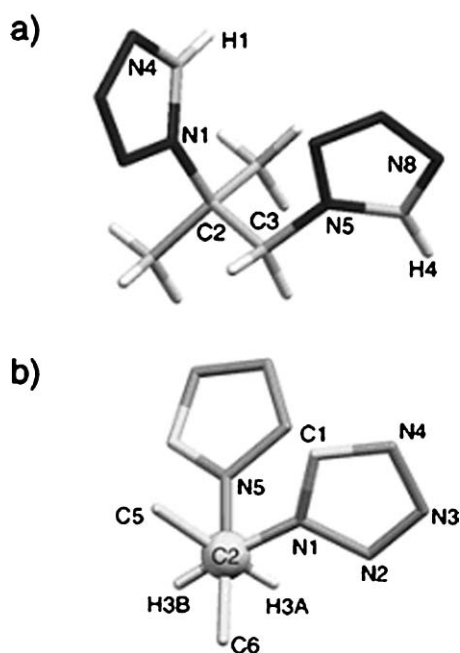
Fig. 1 (a) View of the solid-state conformation of btzmp and (b) view of the Newman projection along the C2–C3 bond.

Experimental

Elemental analysis (C, H, N, S) was performed on a Perkin-Elmer 2400 series II at the Gorlaeus Laboratories. UV-Vis spectra were obtained on a Perkin-Elmer Lambda 900 spectrophotometer using the diffuse reflectance technique, with MgO as a reference. A sample holder mounted on a Dewar and in thermal contact with the refrigerant through a copper rod was used to perform measurements at temperatures around 100 K. The spectral range used was 200–1200 nm. All samples, crystalline or powder, were crushed when placed in the sample holder. Magnetic suscepti-bility measurements were carried out using a Quantum Design MPMS-5 S SQUID magnetometer. The SQUID probes the total magnetisation of the sample by measuring the induced currents in

a Josephson junction when moving the sample in between coils. The accessible field is up to 5 T, and the temperature ranges from 1.8 to 400 K. The data were measured at 1000 G from 4 to 300 K. Data were corrected for magnetisation of the sample holder and for the diamagnetic contributions, which were estimated from the Pascal's tables.[17] Samples made out of single crystals were gently crushed prior to measurement. ^{57}Fe Mössbauer spectra were recorded between 4.2 and 294 K in transmission geometry with a constant acceleration spectrometer using a ^{57}Co**Rh** source, relative to which all centre shifts, δ, are given, and a continuous flow cryostat with a temperature stability of ± 0.5 K. To avoid a possible temperature hysteresis spectra were taken both during increasing temperature (heating mode) and decreasing temperature (cooling mode). For the analysis, the full Hamiltonian was solved, taking into account also the sample thickness. X-Ray data for btzmp were collected at 150 K on a Nonius KappaCCD diffractometer using a rotating anode with graphite-monochromated Mo Kα radiation ($\lambda = 0.71073$ Å). The structure was solved with the direct methods program SHELXS86[18] and refined on F^2 with SHELXL-97.[19] H atoms were included in the refinement at calculated positions and refined riding on the atoms to which they are attached with standard geometry and isotropic displacement parameter constraints from SHELXL-97.[19] CCDC reference number 650322. X-ray data for **1** were collected at 200 and 100 K, with the same instrumentation and software as for btzmp.[20] The perchlorate anion was included with a two-site disorder model for the 200 K structure. CCDC reference numbers 650323 and 650324, respectively.

Syntheses

Btzmp; 1,2-bis(tetrazol-1-yl)-2-methylpropane. btzmp was synthesised according to the procedure reported by Kamiya and Saito.[21] 0.056 mol (4.94 g) of 2-methylpropane-1,2-diamine, 0.113 mol (7.35 g) of sodium azide, and 0.57 mol of triethylortho-formate (84.47 g) were dissolved in 100 ml of acetic acid, and stirred at 90 °C for at least 12 h. The solvent was removed under reduced pressure and a white solid, *i.e.* the crude compound precipitated. The solid material was then washed with water and the product was air-dried. Yield: 9.33 g (65%). ^{1}H NMR (300 MHz, CD$_3$OD): δ 1.8 (s, 6H, (*CH$_3$*)$_2$–C), 5 (s, 2H, (C–*CH$_2$*–ttz), 8.9 (s, 1H, ttz), 9.1 (s, 1H, ttz) ppm. IR: $v = 3132.5$ cm^{-1} (v_{Cttz-H}). Anal. Calcd. (found) for C$_6$H$_{10}$N$_8$: C, 37.11 (36.6)%; H, 5.19 (5.64)%; N 57.7 (57.19)%.

[Fe(μ-btzmp)$_2$(btzmp)$_2$](ClO$_4$)$_2$ (1). One equivalent of btzmp (0.10 g, 0.5 mmol) was dissolved in 10 ml of methanol in an Erlenmeyer. One equivalent of Fe(ClO$_4$)$_2$·4H$_2$O (0.13 g, 0.5 mmol) was dissolved in 5 ml of methanol containing approximately 20 mg of ascorbic acid. The iron(II) solution was added to the ligand solution, and the resulting mixture was heated to 50 °C for 2 h. Afterwards, the complex solution was left unperturbed for one week at room temperature allowing slow evaporation of the solvent. As soon as the compound started to crystallise (when almost all the solvent had evaporated), the Erlenmeyer was closed, and the solution was left unperturbed for another two days. The title compound was then filtered, and was washed with 20 ml of methanol. Yield = 10%. IR (v, cm^{-1}): 3130 (vCttz–H), 1084 (vCl–O) Anal. Calcd. (found) for C$_{24}$H$_{40}$C$_{12}$FeN$_{32}$O$_8$: C, 27.94 (28.22)%; N, 43.45 (43.66)%; H, 3.91 (3.80)%.

Table 1 Crystallographic data for the free ligand btzmp (1,2-bis(tetrazol-1-yl)-2-methylpropane)

	btzmp
Formula	$C_6H_{10}N_8$
Fw/g mol^{-1}	194.2
Crystal system	Monoclinic
Space group	$P2_1/c$
a/Å	8.3070(10)
b/Å	9.2546(10)
c/Å	13.0534(9)
β/°	119.423(5)
V/Å³	874.08(16)
Z	4
ρ_{calcd}/g cm^{-3}	1.476
T/K	150(K)
2θ max/°	54.8
Nr of reflections	13630
Nr of unique reflections	1980
R(int)	0.063
No of observed reflections	1695
R ($I > 2\theta(I)$)	0.0348
$wR2$	0.0873
S	1.07
Crystal shape	Cube
Colour	White

Table 2 Crystallographic data for complex **1**. When the parameters depend on the temperature, they are entered in the order 200 K and 100 K

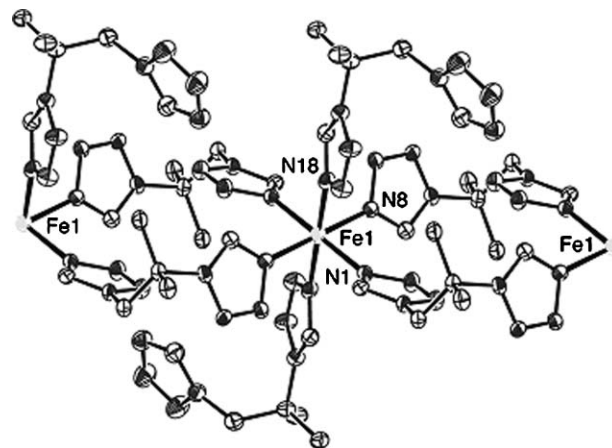|	$[Fe(\mu\text{-btzmp})_2(\text{btzmp})_2](ClO_4)_2$
Formula	$C_{24}H_{40}Cl_2FeN_{32}O_8$
FW/g mol^{-1}	1031.63
Crystal system	Triclinic
Space group	P-1
a/Å	8.5157(15); 8.3039(15)
b/Å	11.1223(18); 10.9503(18)
c/Å	12.432(2); 12.311(2)
α/°	79.24(2); 79.38(2)
β/°	78.96(2); 83.69(3)
γ/°	74.62(4); 73.65(4)
V/Å³	1102.8(4); 1053.8(4)
Z	2
ρ_{calcd}/g cm^{-3}	1.5534(6); 1.6256(6)
T/K	200; 100
2θ max/°	50.5; 50.5
No of reflections	13912; 12659
No of unique reflections	3961; 3788
R(int)	0.078; 0.0672
No of observed reflections	2648; 2741
R ($I > 2\theta(I)$)	0.0590; 0.0591
$wR2$	0.1601; 0.1320
S	1.02; 1.04
Crystal shape	Hexagon
Colour	White; Purple

Results

Crystal Structure of the btzmp ligand

The ligand btzmp crystallises in methanol as colourless blocks (Table 1). The solid-state conformation of btzmp is depicted in Fig. 1, together with a Newman projection. The methyl substituents favour a *gauche* conformation. On the contrary, a *trans* conformation is observed for the free endi ligand,[13] which does not have hindering methyl groups. In addition, the bulkiness of the methyl groups tilts the tetrazole planes to an angle of 57.28(7)° with respect to each other. These steric constraints result in a particular crystal packing (Fig. S1)‡ in which the atoms H4 and H1 of the tetrazole rings are involved in hydrogen bonds (H4···N4 = 2.38 Å and H1···N8 = 2.54 Å) with tetrazole units of adjacent molecules. Contrary to the tetrazole rings of the free endi ligand,[13] the heteroaromatic rings of btzmp are not π–π stacked.

Crystal structure of $[Fe(\mu\text{-btzmp})_2(\text{btzmp})_2](ClO_4)_2$. Compound **1** crystallises in the *P*-1 space group and was studied both at 100 and 200 K (Table 2). The iron(II) ion is located on a crystallographic inversion centre. The unit cell is composed of an Fe^{II} ion, two perchlorate anions and four btzmp ligands. One btzmp is acting as a bridging ligand, while the other is monocoordinated to an iron ion. At 200 K, the perchlorate anion is disordered over two positions (0.542(4):0.458(4)), while at 100 K no disorder is observed. The coordination sphere is constituted of 6 tetrazole rings coordinated through their N_D atom, forming a slightly distorted octahedral environment (see Fig. 2). As expected,[22] the distortion of the octahedron decreases when going to the LS state (Table 3). To evaluate the octahedral distortion,[22] the parameter Σ has been considered.§ Thus, the geometry of

Fig. 2 Labelled ORTEP representation (at the 50% probability level) of $[Fe(\mu\text{-btzmp})_2(\text{btzmp})_2](ClO_4)_2$(**1**).

the HS state of **1** shows the largest octahedral distortion so far observed for tetrazole-based compounds (23.6°).[23] In its LS state,

Table 3 Selected interatomic distances [Å] and angles [°] for (**1**). a = −1 + x, y, z; c = −x, −y, 2 − z; d = 1 − x, −y, 2 − z.

$[Fe(\mu\text{-btzmp})_2(\text{btzmp})_2](ClO_4)_2$	200 K	100 K
Fe1–N1	2.181(3)	2.0005(29)
Fe1–N18	2.207(4)	2.0021(25)
Fe1–N8a	2.171(3)	1.9864(30)
N1–Fe1–N18	92.65(14)	91.44(12)
N1–Fe1–N8a	87.04(13)	88.12(12)
N1–Fe1–N18c	87.35(14)	88.56(12)
N1–Fe1–N8d	92.96(13)	91.88(12)
N18–Fe1–N8a	89.70(14)	90.58(12)
N18–Fe1–N8d	90.30(14)	89.42(12)

§ Σ symbolizes the sum of the deviations from 90° of the 12 *cis* N–Fe–N angles.

1 exhibits a much smaller octahedral distortion (15.6). The Fe–N distances at 200 K are 2.207(4) (Fe–N18), 2.181(4) (Fe–N1) and 2.171(3) Å (Fe–N8), falling in the expected range for a HS Fe^{II} centre (see Table 3).[2] It is noticeable that the Fe–N distances for monocoordinated ligands are approximately 0.02 Å longer, compared to those of bridging tetrazole ligands. At 100 K, the Fe–N distances decrease by a factor of around 9%. The observed values of 2.002(3) (Fe–N18), 2.001(3) (Fe–N1) and 1.986(3) Å (Fe–N8) are thus normal for LS Fe^{II} centres (see Table 3).[2] The change in the metal-to-ligand bond length affects the angles of the coordinated tetrazole rings. A considerable modification of the [tetrazole-centroid]–N_D–Fe angle is occurring upon the spin transition. This angle characterises the tilting of the whole tetrazole ring with respect to the Fe^{II} metal ion. The increase of this angle in the low-spin state thus suggests that the tetrazole rings tend to open up in order to compensate for the decrease of the Fe–N distances (see Fig. 3). This change in the [tetrazole-centroid]–N_D–Fe angle is only observed for the tetrazole ring connected to the $–CH_2–$, which again reflects the steric hindrance caused by the two methyl substituents.
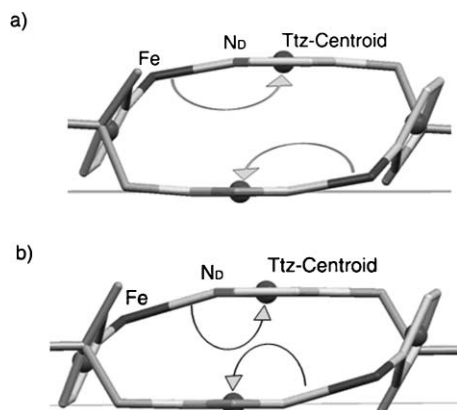

Fig. 3 [Tetrazole-centroid]–N_D–Fe angle for the bridging btzmp ligands of compound **1** (a) in the LS (170.36°) and (b) HS state (163.82°). Non-bridging btzmp ligands and counterions have been omitted for clarity.

Surprisingly, only two of the btzmp ligands extend the overall structure along the *a* axis, while the other two only act as *trans* monodentate ligands. This coordination mode contrasts with those observed for other bistetrazole-based 1D polymers, in which the iron(II) centres are triply bridged, and present no monocoordinated azole ligands.[24] The presence of a double bridge, instead of the typical triple bridge, affects the intrapolymeric distance (namely the Fe–Fe separation in the polymeric chain), which is 8.5157(15) Å at 200 K. This distance is about 1 Å longer than those found for the related [Fe(endi)$_3$](BF$_4$)$_2$ and [Fe(btzp)$_3$](ClO$_4$)$_2$ 1D polymers (see Discussion section).[12,13] The change in spin state results in a decrease of 0.212 Å of the Fe···Fe intrapolymeric distance. Additionally, these monocoordinated ligands have an effect on the crystal packing of [Fe(μ-btzmp)$_2$(btzmp)$_2$](ClO$_4$)$_2$, which does not show the typical hexagonal motif usually observed for bistetrazole-based 1D polymers.[24] In **1**, each polymeric chain is surrounded by six other chains with the anions occupying the ensuing voids (Fig. S2).§ The interpolymeric distances are 11.1223(18) Å and 12.432(2) Å in the HS state and 10.9503(18) Å and 12.311(2) Å in the LS state. No solvent molecules are present

in the crystal lattice, which is a characteristic feature of such 1D bistetrazole spin-transition materials.[23]

Magnetic susceptibility

Compound **1** crystallises as colourless small single crystals. For [tetrazole-Fe^{II}]-based materials, white/colourless crystals generally indicate an HS state at room temperature. Indeed, as shown in Fig. 4, at 300 K $\chi_m T = 3.11$ cm^3 mol^{-1} K^{-1}, implying that the compound is mainly in its HS state. No change is observed until around 135 K where the LS state becomes abruptly populated ($T_{1/2}$ = 133 K). The transition takes place for 98% ($\chi_m T = 0.073$ cm^3 mol^{-1} K^{-1}) of the Fe^{II} centres, 2% remaining HS through the whole temperature range.
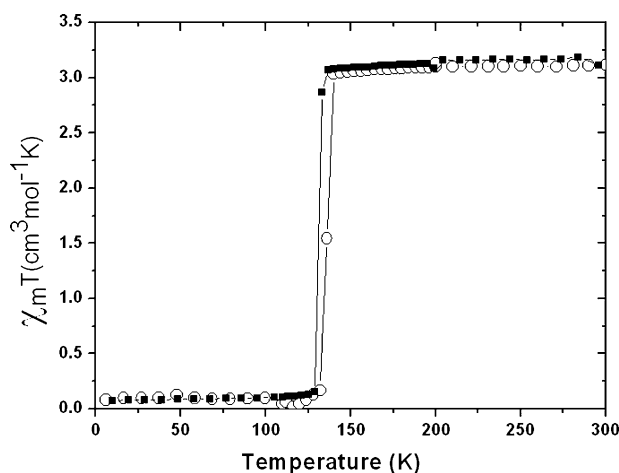

Fig. 4 Plot of $\chi_m T$ *vs.* T for a crystalline sample of [Fe (μ-btzmp)$_2$ (btzmp)$_2$](ClO$_4$)$_2$ (**1**), recorded both in the cooling mode (black squares) and in the heating mode (white circles).

A drastic colour change, from colourless to purple, accompanies the HS → LS transition. As the temperature is increased, a hysteresis loop with a width of about 3 K ($T_{1/2}\uparrow$ = 136 K and $T_{1/2}\downarrow$ = 133 K) is detected, as clearly visible in Fig. 4. The process shows no exhaustion and the hysteresis is reproducible over several cooling/heating cycles (5 cycles).

[57]Mössbauer spectroscopy

The spin transition has been investigated by Mössbauer spectroscopy. In Fig. 5, four significant Mössbauer spectra are depicted. From room temperature to 250 K (Fig. 5), the Mössbauer data do not significantly change. A main signal is observed with quadrupole splitting (1.78–2.0 mm s^{-1}) and isomer shift (0.96 mm s^{-1}) values typical of high spin Fe^{II} centres (Table 4).[25] In addition, a smaller HS signal corresponding to less than 10% of the total iron(II) centres is detected. This signal corresponds to an impurity (which may be ascribed to the polymer chain-ends), and does not vary in intensity throughout the whole temperature range. As the temperature is lowered to 135 K, no significant changes are observed for both signals. At 130 K, a new signal with a quadrupole splitting of 0.20 mm s^{-1} and an isomer shift, δ, of 0.44 mm s^{-1} is detected, which is typical of LS Fe^{II} ions (Table 4).[25] The decrease in intensity of the HS signal with concomitant increase of the LS signal (see HS/LS percentages, Fig. 5) can
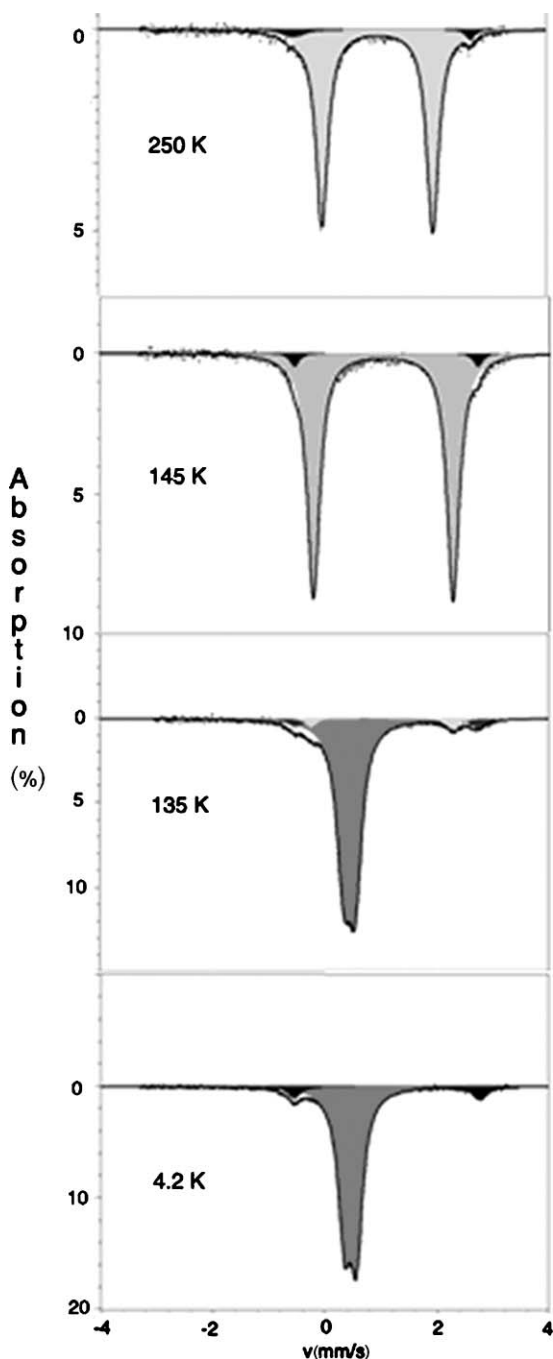
Fig. 5 Selected ^{57}Fe Mössbauer spectra obtained at 250, 145, 135 and 4.2 K in the cooling mode. The LS, HS and HS impurity signals are depicted in dark grey, light grey and black, respectively.

be assigned to the HS → LS spin transition of the Fe centres. The transition temperature falls in the expected range of temperatures observed by magnetic susceptibility. However, the accurate value cannot be given because the data points have been recorded with long temperature intervals. From 130 to 4.2 K no further significant changes are noted, indicating that the spin-crossover process is complete within a range of ≤ 5 K around $T_{1/2}$. For the heating mode, the transition from a low to a high spin state appears between 135 and 140 K, at a few degrees higher than in the

cooling mode, confirming the presence of a hysteresis loop already observed by magnetic susceptibility.

UV-vis-NIR

The diffuse reflectance UV-vis spectra for [Fe(μ-btzmp)$_2$(btzmp)$_2$]-(ClO$_4$)$_2$ show a dependence on the temperature. The spectrum at room temperature (Fig. 6) exhibits a main band centred at 260 nm with a shoulder at 360 nm, corresponding to a metal-to-ligand charge transfer. A second band at 850 nm can be assigned to the $^5T_2 \rightarrow {}^5E$ transition, characteristic of Fe^{II} HS compounds. The spectrum at 77 K (Fig. 6) illustrates a shift of the metal-to-ligand charge transfer band to higher wavelengths ($\lambda = 316$ nm), and the appearance of two new bands at 383 and 551 nm. These two absorption bands correspond to the $^1A_1 \rightarrow {}^1T_2$ and the $^1A_1 \rightarrow {}^1T_1$ transitions, respectively, and are distinctive of LS Fe^{II} compounds.[2] The absorption band at 383 nm seems to be already present at room temperature, as a shoulder on the 260 nm band. At 77 K, the band ascribed to the $^5T_2 \rightarrow {}^5E$ transition in Fe^{II} HS systems is significantly less intense; the occurrence of this absorption at this temperature is most likely due to HS impurities, already observed by Mössbauer spectroscopy. Unfortunately, the irradiation with green light ($\lambda = 559$ nm) in the SQUID cavity at 10 K, did not result in a detectable population of the HS metastable state (*i.e.* the so-called LIESST effect[26] was not observed). No further work has been done to determine the reason for the lack of LIESST, although the steep transition may in part be responsible.
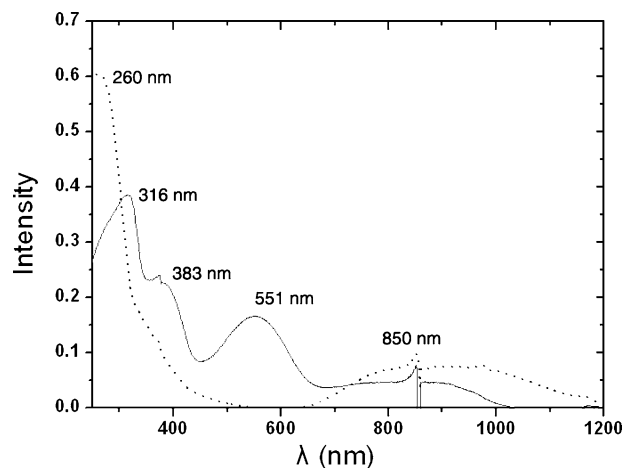
Fig. 6 UV-vis-NIR spectra for compound **1** at room temperature (dotted line) and at liquid nitrogen temperature (full line).

Discussion

The btzmp ligand completes the endi–btzp series. Indeed, all these ligands possess a C2 bridge, differently substituted. The reaction of these ligands with different Fe^{II} salts results in 1D polymers. For [Fe(btzp)$_3$](ClO$_4$)$_2$, the *syn* conformation of the ligand has been suggested as the origin for its dimensionality.[12]

This spatial arrangement, in which the tetrazole rings are almost eclipsed (Newman projection), is also observed for [Fe(endi)$_3$](BF$_4$)$_2$. In contrast, the solid-state structure of [Fe(μ-btzmp)$_2$(btzmp)$_2$](ClO$_4$)$_2$ reveals a *gauche* conformation of the tetrazole rings. Consequently, the nitrogen-donor atoms are

Table 4 Mössbauer spectral hyperfine parameters for complex [Fe(μ-btzmp)₂(btzmp)₂](ClO₄)₂

Temperature/K (heating)	LS component			HS component			HS residual		
	δ[mm s^{-1}]	Δ[mm s^{-1}]	LS fract.	δ[mm s^{-1}]	Δ[mm s^{-1}]	HS fract.	δ[mm s^{-1}]	Δ[mm s^{-1}]	Residual fract.
4.2	0.45(14)	0.21(1)	0.92	—	—	—	1.10(61)	3.3(12)	0.08
130	0.44(1)	0.20(1)	0.93	1.04(1)	2.65(1)	0.02	1.08(1)	3.3(36)	0.06
135	0.44 (1)	0.20(1)	0.89	1.03(1)	2.53(1)	0.05	1.10(1)	3.2(32)	0.06
145	—	—	—	1.03(1)	2.48(1)	0.94	1.10(12)	3.3(24)	0.06
294	—	—	—	0.94(1)	1.78(1)	0.96	1.00(41)	3.1(82)	0.04
Temperature/K (cooling)	**LS component**			**HS component**			**HS residual**		
294	—	—	—	0.95(14)	1.80(28)	0.99	1.0(40)	3.2(81)	0.01
135	—	—	—	1.03(11)	2.49(20)	0.97	1.1(4)	3.3(7)	0.03
127	0.44(30)	0.20(20)	0.93	1.0(12)	2.6(24)	0.03	1.07(94)	3.3(19)	0.04
111	0.45(27)	0.20(15)	0.96	—	—	—	1.1(1)	3.3(3)	0.04

pointing towards different directions, which is reflected in a longer $N_D \cdots N_{D}'$ distance (endi, 5.107 Å; btzp, 5.038 Å and btzmp, 5.687 Å). However, the dimensionality, *i.e.* 1D linear chain, of the compound is not affected by the different ligand conformation. Interestingly, the disposition adopted by the bridging btzmp ligands in compound **1** is also observed in the crystal structure of the free ligand. Apparently, it is not the coordination to the metal ions that determines the conformation of the ligand, as observed for endi. The second methyl substituent most likely forces the ligand to adopt a special spatial arrangement which affects the disposition of the tetrazole rings.

As stated above, the dimensionality of the compound is not influenced by the specific conformation of the btzmp ligand. However, it appears that the steric hindrance, owing to the additional methyl group, determines the number of ligands bridging the Fe^{II} centres. Indeed, for both coordination compounds [Fe(btzp)₃](ClO₄)₂ and [Fe(endi)₃](BF₄)₂, the Fe^{II} centres are triply bridged by their corresponding ligands, while in [Fe(μ-btzmp)₂(btzmp)₂](ClO₄)₂, the iron ions are doubly bridged. This steric effect is again evidenced by the fact that, contrary to endi and btzp which present disorder when coordinated, btzmp shows only one stable position of its bridging mode upon coordination. The two btzmp molecules acting as monodentate ligands consequently modify the crystal packing, which differs notably from those of [Fe(btzp)₃](ClO₄)₂ and [Fe(endi)₃](BF₄)₂.[12,13] The different solid-state packing is reflected in longer interpolymeric distances and shorter intrapolymeric distances for compound **1**.[23]

The structural modifications occurring during the spin transition are distinct for each compound. Compound **1** shows the largest alterations of the metal to ligand distances, while [Fe(btzp)₃](ClO₄)₂ has the smallest variations of these bond lengths. Surprisingly, for the btzp derivative, the change in bond length does not structurally modify the ligand. In the case of endi, a variation of the torsion angle is observed, which amounts to 7°. This different response of the ligands to the decrease of the Fe–N distances does not appear to affect the spin-crossover properties of the corresponding materials, as they both show gradual HS → LS transitions at similar temperatures. In compound **1**, the torsion angle does not significantly vary (a minor variation of about 1° is observed). However, a structural change is noted for the ligand btzmp with the spin crossover. The [ttz-centroid]–N$_D$–Fe angle diverges by almost 6° from the HS to the LS forms. In

1D bistetrazole-based SCO coordination polymers, this angle is usually larger for the LS compound.[23] This increase suggests that the tetrazole rings "open up" to counterbalance the shortening of the Fe–N distances. The adjustment of the [ttz-centroid]–N$_D$–Fe angle is especially large for compound **1**, while it is almost insignificant for the other two complexes. The increase of the [ttz-centroid]–N$_D$–Fe angle has a drastic effect on the disorder of the perchlorate anions. At high temperatures, the ClO₄⁻ ions are disordered and involved in weak anion–π interactions[27,28] with the tetrazole rings. Upon the HS → LS transition, the tetrazole rings "open up", *i.e.* the [ttz-centroid]–N$_D$–Fe angle increases, which results in closer contacts with the perchlorate anions (no positional shift of the anion is detected). Accordingly, the anion–π interactions strengthen (shorter anion ⋯ centroid separations), with concomitant loss of disorder.

The magnetic susceptibility measurements reveal that the spin-transition phenomenon detected in **1** presents a hysteresis loop of 3 K. The HS ↔ LS transition is much steeper than the ones observed for [Fe(btzp)₃](ClO₄)₂ and [Fe(endi)₃](BF₄)₂. Abrupt transitions are commonly assigned either to highly cooperative systems,[2] or to compounds which present a crystallographic phase transition.[6,29,30] The main structural differences between the SCO coordination polymers obtained from the ligands endi, btzp, and btzmp are found in their respective crystal packing. The steric bulk of the non-bridging btzmp ligands present in compound **1** generates a different packing of the polymer chains, possibly giving rise to a more rigid and compact framework. This increased rigidity would induce a higher cooperativity, and thus the occurrence of a hysteresis loop. The thermal order/disorder transition observed with the perchlorate anions may also cause the abrupt spin-state change. It appears that the spin transition is related to the order/disorder transition of the anions in the lattice. This affirmation, although speculative, is based on the X-ray structural data. The aforementioned variation of the [ttz-centroid]–N$_D$–Fe angle during the spin transition observed for all 1D SCO materials, in this case strengthens the anion–π interactions and favours just one position of the anion in the crystal lattice at 100 K. Nevertheless, both structural transformations, *i.e.* adjustment of the tetrazole plane–iron angle with the consecutive ordering of the ClO₄⁻ ions, are most likely involved in the abruptness of the transition. The transition temperature $T_{1/2}$ determined by Mössbauer spectroscopy is comparable to the one obtained by magnetic

susceptibility measurements. [57]Fe Mössbauer measurements also reveal the presence of a small amount of, probably end-of-chain, HS iron(II) impurities.

Conclusions

The incorporation of an additional methyl substituent on the backbone of the spacer separating the tetrazole rings, *i.e.* the ligand btzmp, significantly affects the solid-state arrangement of the ligand in comparison with the original ligands endi and btzp. As a result, the iron(II) polymer chains obtained from this btzmp ligand exhibit a notably distinct crystal packing, compared to the earlier reported, related materials prepared from the less hindered ligands endi and btzp. Indeed, the presence of two additional methyl substituents in btzmp most likely decreases the flexibility of the ligand, thus affecting its coordinating properties. These new coordination features have an effect on the structural changes caused by the spin transition, and thus on its spin-transition properties. The combined structural variations, namely the adjustment of the [ttz-centroid]–N_D–Fe angle to counteract the variations of the Fe–N separations, and the thermal order/disorder of the ClO_4^- anions, appear to produce an abrupt spin transition, with occurrence of a small hysteresis loop. A simple increase in rigidity of the overall network is not excluded.

Acknowledgements

Notes and references

1 O. Kahn, J. Kröber and C. Jay, *Adv. Mater.*, 1992, **4**, 718–728.
2 P. Gütlich, A. Hauser and H. Spiering, *Angew. Chem., Int. Ed. Engl.*, 1994, **33**, 2024.
3 J. K. Beattie, Dynamics of Spin Equilibria in Metal-Complexes, in *Advances in Inorganic Chemistry*, Elsevier, Amsterdam, 1988, vol. 32, pp 1–53.
4 A. Hauser, P. Gütlich and H. Spiering, *Inorg. Chem.*, 1986, **25**, 4245–4248.
5 H. Spiering, Elastic interaction in spin crossover compounds, in *Spin Crossover in Transition Metal Compounds III, Topics in Current Chemistry*, ed. P. Gütlich and H. A. Goodwin, Springer, Heidelberg, 2004, vol. 235, pp 171–195.
6 E. König, G. Ritter, S. K. Kulshreshtha, J. Waigel and L. Sacconi, *Inorg. Chem.*, 1984, **23**, 1241–1246.
7 O. Kahn and E. Codjovi, *Philos. Trans. R. Soc. London, Ser. A*, 1996, **354**, 359–379.
8 K. S. Murray, C. J. Kepert, Cooperativity in spin crossover systems: Memory, magnetism and microporosity, in *Spin Crossover in Transition Metal Compounds I, Topics in Current Chemistry*, ed. P. Gütlich and H. A. Goodwin, Springer, Heidelberg, 2004, vol. 233, pp 195–228.
9 S. M. Neville, B. A. Leita, D. A. Offermann, M. B. Duriska, B. Moubaraki, K. W. Chapman, G. J. Halder and K. S. Murray, *Eur. J. Inorg. Chem.*, 2007, 1073–1085.
10 M. Quesada de la, V. A. Pena-O'Shea, G. Aromi, S. Geremia, C. Massera, O. Roubeau, P. Gamez and J. Reedijk, *Adv. Mater.*, 2007, **19**, 1397–1402.
11 C. M. Grunert, J. Schweifer, P. Weinberger, W. Linert, K. Mereiter, G. Hilscher, M. Müller, G. Wiesinger and P. J. van Koningsbruggen, *Inorg. Chem.*, 2004, **43**, 155–165.
12 P. J. van Koningsbruggen, Y. Garcia, O. Kahn, L. Fournès, H. Kooijman, A. L. Spek, J. G. Haasnoot, K. Moscovici, K. Provost, A. Michalowicz, F. Renz and P. Gütlich, *Inorg. Chem.*, 2000, **39**, 1891–1900.
13 J. Schweifer, P. Weinberger, K. Mereiter, M. Boca, C. Reichl, G. Wiesinger, G. Hilscher, P. J. van Koningsbruggen, H. Kooijman, M. Grunert and W. Linert, *Inorg. Chim. Acta*, 2002, **339**, 297–306.
14 P. J. van Koningsbruggen, M. Grunert and P. Weinberger, *Monatsh. Chem.*, 2003, **134**, 183–198.
15 A. Absmeier, M. Bartel, C. Carbonera, G. N. L. Jameson, P. Weinberger, A. Caneschi, K. Mereiter, J. F. Létard and W. Linert, *Chem.–Eur. J.*, 2006, **12**, 2235–2243.
16 P. J. van Koningsbruggen, Y. Garcia, H. Kooijman, A. L. Spek, J. G. Haasnoot, O. Kahn, J. Linarès, E. Codjovi and F. Varret, *J. Chem. Soc., Dalton Trans.*, 2001, 466–471.
17 O. Kahn, Molecular Magnetism, in *Molecular Magnetism*, VCH, New York, 1993, p 131.
18 G. M. Sheldrick, *SHELXS, 86*, University of Göttingen, 1986.
19 G. M. Sheldrick, *SHELXL-97 Program for Crystal Structure Refinement*, Universityof Göttingen, 1997.
20 A. L. Spek, *J. Appl. Crystallogr.*, 2003, **36**, 7–13.
21 T. Kamiya and Y. Saito, *Ger. Offen.*, 1973, 2147023.
22 P. Guionneau, M. Marchivie, G. Bravic, J. F. Létard, D. Chasseau, Structural aspects of spin crossover. Example of the (FeLn)-L-II(NCS)(2) complexes, in *Spin Crossover in Transition Metal Compounds II*, ed. P. Gütlich and H. A. Goodwin, 2004, vol. 234, pp 97–128.
23 M. Quesada, *Spin-Transition Frameworks based on Bistetrazole and Triazine Ligands*, PhD Thesis, Leiden University, Leiden, 2007.
24 P. J. van Koningsbruggen, Special classes of iron(II) azole spin crossover compounds, in *Spin Crossover in Transition Metal Compounds I, Topics in Current Chemistry*, ed. P. Gütlich and H. A. Goodwin, Springer, Heidelberg, 2004, pp 123–149.
25 E. König, G. Ritter and H. A. Goodwin, *Chem. Phys.*, 1973, **1**, 17–26.
26 S. Decurtins, P. Gütlich, C. P. Köhler, H. Spiering and A. Hauser, *Chem. Phys. Lett.*, 1984, **105**, 1–4.
27 P. Gamez, T. J. Mooibroek, S. J. Teat and J. Reedijk, *Acc. Chem. Res.*, 2007, DOI: 10.1021/ar7000099.
28 D. Quiñonero, C. Garau, C. Rotger, A. Frontera, P. Ballester, A. Costa and P. M. Deyà, *Angew. Chem., Int. Ed.*, 2002, **41**, 3389–3392.
29 O. Roubeau, *Solid, State Properties of Triazole-Based Fe(II) Materials*, PhD thesis, Leiden University, Leiden, 2002.
30 O. Roubeau, P. C. M. Gubbens, D. Visser, M. Blaauw, P. D. de Reotier, A. Yaouanc, J. G. Haasnoot, J. Reedijk, S. Sakarya, U. A. Jayasooriya, S. P. Cottrell and P. J. C. King, *Chem. Phys. Lett.*, 2004, **395**, 177–181.